

# Fractals in petrology

Donald L. Turcotte\*

*Department of Earth and Atmospheric Sciences, Cornell University, Ithaca, NY 14853, USA*

Received 14 November 2001; accepted 10 June 2002

---

## Abstract

A fractal (power-law) distribution is the only statistical distribution applicable to a scale-invariant process. One of the major problems in petrology is the distribution of trace elements in the Earth's crust. Extreme values of this distribution result in ore deposits. There is accumulating observational evidence that tonnage–grade statistics of ore deposits are often fractal (power-law). Rayleigh distillation and chromatographic models can explain power-law (fractal) distributions for the extreme values of trace element concentrations. An alternative fractal approach to problems in petrology is to use self-affine fractals. The standard approach is to take a Fourier transform of a continuous signal (an example would be the concentration of a mineral along a linear track). If the Fourier coefficients scale as a power-law of the wavelength, the distribution is a self-affine fractal. Many well logs give this result. Multifractal analyses can also be applied to problems in petrology.

© 2002 Elsevier Science B.V. All rights reserved.

*Keywords:* Fractals; Petrology; Self-similarity; Ore deposits; Textures

---

## 1. Introduction

The concept of fractals was introduced by Mandelbrot (1967) in terms of the length of the coast of Britain. The length of the coast is obtained using a measuring rod of a specified length. The length of a rocky coastline is well-approximated by a power-law dependence on the length of the measuring rod; the power determines the fractal dimension of the coastline. It is not possible to obtain a specific value for the length of a coastline due to the many small indentations as small as millimeters or less. To a good approximation a rocky coastline is a statistical, self-

similar fractal. An example of a deterministic self-similar fractal is the Koch triadic island illustrated in Fig. 1. The construction starts with an equilateral triangle at zero order (Fig. 1a). At second order smaller equilateral triangles are placed at the center of each side (Fig. 1b). As the construction is extended to infinite order, the length of the perimeter goes to infinity. For this construction, the length of the perimeter of the figure, at any order, scales exactly as a power-law of the inverse of the length of a side (Turcotte, 1997, p. 11).

A power-law (fractal) distribution is the only statistical distribution that is scale-invariant. Other distributions such as the Gaussian (normal) and log-normal require a characteristic length or time in their definition. There are many examples of scale-invariant (power-law) distributions in geology. Examples

---

\* Tel.: +1-607-254-7282; fax: +1-607-254-4780.

E-mail address: turcotte@geology.cornell.edu (D.L. Turcotte).

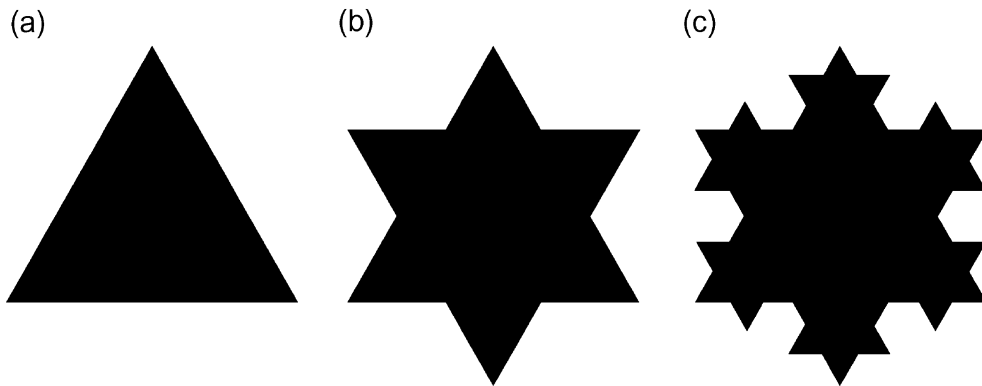


Fig. 1. The triadic Koch island. (a) An equilateral triangle with sides  $r_0 = 1$ . (b) Three triangles with sides  $r_1 = 1/3$  are added. (c) Twelve triangles with sides  $r_2 = 1/9$  are added. The perimeters  $P_0 = 3$ ,  $P_1 = 4$ ,  $P_2 = 16/3$  satisfy the relation  $P_i = 3r_i^{-0.262}$ .

include the frequency size distribution of earthquakes and drainage networks, among many others (Korvin, 1992; Turcotte, 1997).

## 2. Mineral deposits

One of the fundamental problems in geology is the statistical distribution of chemical elements in the Earth's crust. Extreme concentrations of elements lead to ore deposits. The statistical distribution of minerals in ore deposits plays a fundamental role in economic geology. This is generally expressed in terms of tonnage–grade statistics. But ore deposits are only one aspect of the broader questions regarding the statistical distributions of trace elements as a whole. As in other applications of geostatistics the major alternative distributions are log-normal and power-law (fractal). Turcotte (1986), following the work of Cargill et al. (1980, 1981) and Cargill (1981), has argued that ore deposits satisfy fractal statistics. Ahrens (1954a,b, 1963a,b) and Vistelius (1960) have argued that trace elements universally satisfy log-normal statistics. Allègre and Lewin (1995) argue that the applicability of the two distributions depends upon the fundamental geochemical processes responsible for the concentrations of the trace elements. If the dominant process is mixing, normal distributions result; if the dominant process is differentiation, power-law (fractal) or log-normal distributions may result.

In general, power-law distributions cannot be applicable at all scales. Pure power-law distributions diverge either at the largest or smallest scales. However, in many applications we are concerned about the extreme value statistics. Do the extreme values satisfy exponential (thin tail) statistics or power-law (fat tail) statistics? The extreme value statistics for log-normal distributions are intermediate but tend towards a thin tail limit.

An example of extreme values in element distributions is ore deposits. Whether ore deposits satisfy thin tail or fat tail extreme value statistics has very large implications regarding potential ore reserves.

The classic definition of a self-similar fractal is

$$N_i = \gamma r_i^{-D} \quad (1)$$

where  $N_i$  is the number of objects with a size  $r_i$ ,  $D$  is the fractal dimension, and  $\gamma$  is a constant. An example of a self-similar fractal construction in three dimensions is the Menger sponge illustrated in Fig. 2. A zero-order solid cube ( $N_0 = 1$ ) with unit dimensions ( $r_0 = 1$ ) is considered as illustrated in Fig. 2a. This unit cube is then divided into 27 cubes each with  $r_1 = 1/3$ . At first order, the six cubes at the center of each side are removed as well as the center cube. Twenty solid cubes remain with  $r_1 = 1/3$  so that  $N_1 = 20$  as illustrated in Fig. 2b. At second order each of the 20 remaining cubes are divided into 27 cubes each with  $r_2 = 1/9$ . At second order the six cubes at the center of each side are removed as well as the center cube. Four

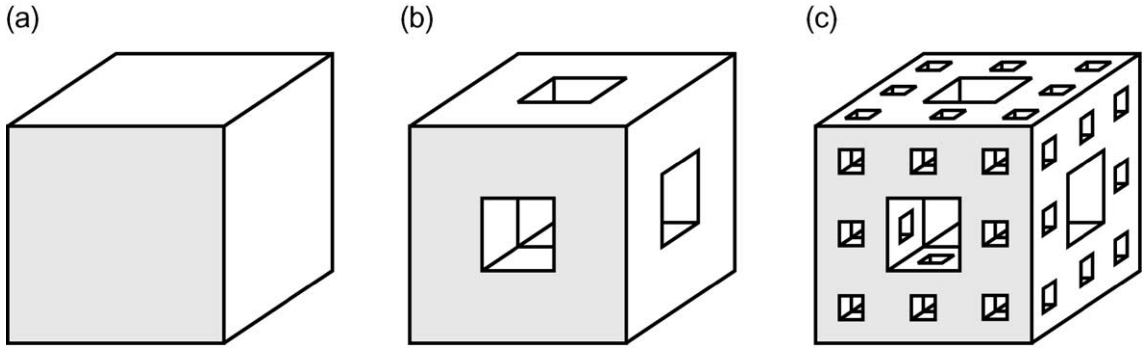


Fig. 2. The Menger sponge. (a) The unit cube  $N_0=1$  with  $r_0=1$ . (b) The unit cube is divided in 27 cubes with  $r_1=1/3$ , 7 are removed so that  $N_1=20$ . (c) Each of the 20 remaining cubes in (b) is divided into 27 cubes with  $r_2=1/9$ , 7 are removed from each of these cubes so that  $N_2=20 \times 20=400$ .

hundred solid cubes remain with  $r_2=1/9$  so that  $N_2=400$  as illustrated in Fig. 2c. From Eq. (1), we find that the fractal dimension of the construction is given by

$$D = \frac{\log(N_{i+1}/N_i)}{\log(r_i/r_{i+1})} = \frac{\log(N_1/N_0)}{\log(r_0/r_1)} \\ = \frac{\log(N_2/N_1)}{\log(r_1/r_2)} = \frac{\log 20}{\log 3} = 2.7268 \quad (2)$$

The construction given in Fig. 2 can be extended to higher and higher orders.

The Menger sponge can be used to illustrate how a fractal tonnage–grade distribution can be obtained as illustrated in Fig. 3. The remaining blocks in the Menger sponge construction are assumed to be the pure mineral,  $C=1$ . The holes in the construction are assumed to be barren country rock,  $C=0$ . A zero-order solid cube is taken to be the pure mineral thus  $C_0=1$  and its mass  $M_0$  (volume  $V_0$ ) is taken to be unity ( $M_0=V_0=1$ ) as illustrated in Fig. 3a. At first order we consider the first-order Menger sponge illustrated in Fig. 2b. This construction is made up of  $N_1=20$  unit cubes of the pure mineral and 7 unit cubes of barren country rock. Thus the mean concentration in this mass (volume) is  $C_1=20/27=0.741$  and its mass  $M_1$  (volume  $V_1$ ) is  $M_1=V_1=3^3=27$ . For simplicity, we assume the density of the mineral and barren country rock is equal. At second order, we consider the second-order Menger sponge illustrated in Fig. 2c. This construction is made up of  $N_2=400$  unit cubes of the

pure mineral and  $20 \times 7 + 7 \times 27 = 329$  unit cubes of barren country rock. Thus the mean concentration in this mass (volume) is  $C_2=400/729=20^2/27^2=0.549$  and its mass  $M_2$  (volume  $V_2$ ) is  $M_2=V_2=9^3=729$ .

We hypothesize that for a fractal tonnage–grade distribution the relation

$$C_i = \mu M_i^{-\alpha} \quad (3)$$

is satisfied where  $\mu$  is a constant. We now show that this relation agrees with the results given above. From Eq. (3), we have

$$\alpha = \frac{\log(C_0/C_1)}{\log(M_1/M_0)} = \frac{\log(C_1/C_2)}{\log(M_2/M_1)} \\ = \frac{\log(27/20)}{\log 27} = 1 - \frac{\log 20}{3 \log 3} \quad (4)$$

Comparing Eqs. (2) and (4), we conclude that

$$\alpha = 1 - \frac{1}{3}D \quad (5)$$

and substitution into Eq. (3) gives

$$C_i = \mu M_i^{-(1-D/3)} \quad (6)$$

This is our basic fractal tonnage ( $M_i$ )–grade ( $C_i$ ) relation. For the example given in Fig. 2, from Eqs. (4) and (5) we have  $\alpha=0.091$  and  $D=\log 20/\log 3=2.7268$  as in Eq. (2). Note that this definition of the fractal dimension differs from the one used by Turcotte (1986, 1997).

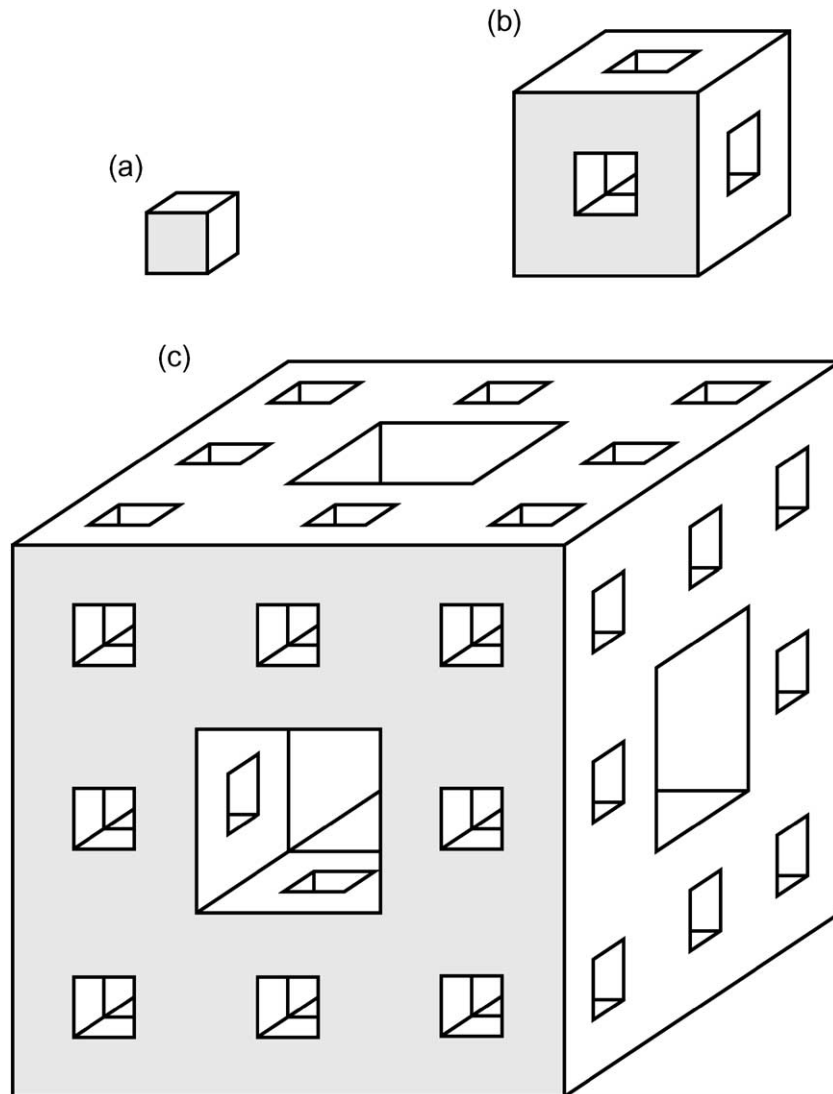


Fig. 3. Menger sponge model for a fractal tonnage grade distribution. (a) A unit cube of the pure mineral,  $M_0 = 1$ ,  $C_0 = 1$ . (b) Twenty unit cubes of the pure mineral and 7 unit cubes of barren country rock,  $M_1 = 27$ ,  $C_1 = 20/27$ . (c) Four hundred unit cubes of the pure mineral and 329 unit cubes of barren country rock  $M_2 = 729$ ,  $C_2 = 400/729$ .

The Menger sponge construction illustrated in Figs. 1 and 2 can be modified to illustrate a range of fractal tonnage–grade distributions. Instead of remaining 20 solid cubes ( $N_i = 20$ ), we retain 2 ( $N_1 = 2$ ), 4 ( $N_1 = 4$ ), and 8 ( $N_1 = 8$ ) cubes. When these values are used in the construction illustrated in Fig. 2, a range of  $\alpha$  values and fractal dimensions  $D$  are obtained. These are tabulated in Table 1. The fractal dimensions are the fractal dimensions of the corre-

sponding Menger sponge construction and range from 0.63 for  $N_1 = 2$  to 2.73 for  $N_1 = 20$  (the true Menger sponge). The power-law exponents  $\alpha$  for the fractal tonnage–grade distributions range from 0.790 for  $N_1 = 2$  to 0.091 for  $N_1 = 20$ .

The Menger sponge used in Figs. 2 and 3 is a deterministic fractal whereas we consider mineral deposits to be statistical fractals. The relation is the same as that between the deterministic triadic Koch

Table 1  
Five examples of the Menger sponge model for fractal tonnage–grade distributions

$N_0$	$M_0$	$C_0$	$N_1$	$M_1$	$C_1$	$N_2$	$M_2$	$C_2$	$\alpha$	D
1	1	1	2	27	2/27	4	729	4/729	0.790	0.63
1	1	1	4	27	4/27	16	729	16/729	0.579	1.26
1	1	1	8	27	8/27	64	729	64/729	0.369	1.89
1	1	1	16	27	16/27	256	729	256/729	0.159	2.52
1	1	1	20	27	20/27	400	729	400/729	0.091	2.73

Island given in Fig. 1 and rocky coastlines. For mineral deposits, we modify the deterministic tonnage grade relation given in Eq. (3) to the form

$$\bar{C} = \mu M^{-\alpha} \tag{7}$$

where  $\bar{C}$  is the mean grade and  $M$  is the ore mass considered.

The subject of tonnage–grade relations for ore deposits has been reviewed by Harris (1984). There is clearly a controversy in the literature between log-normal statistics (Lasky, 1950; Musgrove, 1965) and power-law (fractal) statistics (Cargill et al., 1980,

1981; Cargill, 1981). Results obtained by Cargill (1981) for the tonnage–grade of lode gold in the United States are given in Fig. 4. This correlation was based on records of annual production and mean grade. The cumulative mass of gold mined prior to a specified date was divided by the cumulative mass of ore from which the gold was extracted to give the cumulative mean grade. The data points in Fig. 4 represent the 5-year cumulative mean grade versus the cumulative mass of ore mined. The data correlate with the power-law fractal relation (7) taking  $\alpha=0.517$ . From Eq. (5) the corresponding fractal dimension is  $D=1.45$ .

The working hypothesis is that the ores mined in the earliest time period had the highest grades. As time passed and ore tonnage increased, the ore grade decreased systematically in agreement with Eq. (7). In terms of the deterministic Menger sponge model given in Fig. 3, Fig. 3a is the small tonnage high grade ores, Fig. 3b is the intermediate tonnage intermediate grade ore, and Fig. 3c is the large tonnage low grade ores. Turcotte (1986) also found good fractal correlations with production records for

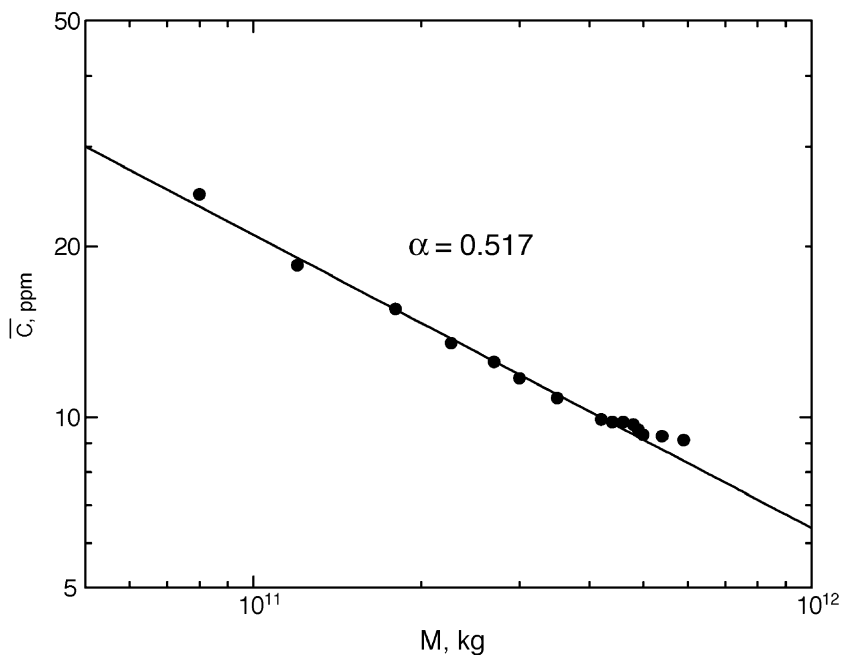


Fig. 4. Dependence of the cumulative ore mass  $M$  on mean grade  $\bar{C}$  for lode gold production in the United States (Cargill, 1981). The data points are production records of the 5-year cumulative average grade  $\bar{C}$  versus the cumulative tonnage of ore  $M$  for the period 1906–1976. The straight-line correlation is with the power-law relation (7) taking  $\alpha=0.517$ .

Table 2  
Fractal correlations of tonnage–grade data given by Cargill et al. (1980, 1981) and Cargill (1981)

Mineral	$\alpha$	D	K
Copper	0.387	1.84	0.61
Uranium	0.490	1.52	0.51
Gold	0.517	1.45	0.48
Mercury	0.660	0.99	0.33

copper, uranium, and mercury. These results are summarized in Table 2. The values of  $\alpha$  range from 0.387 for copper to 0.660 for mercury. A large value of  $\alpha$  implies a strong fractionation of the mineral in the ore.

Spatial distributions of ore deposits have also been shown to satisfy fractal statistics. Carlson (1991) examined the spatial distribution of 4775 hydrothermal precious metal deposits in the western United States and found that the probability–density distribution for these deposits is fractal. Blenkinsop (1994) found similar results for gold deposits in the Zimbabwe Archean craton.

### 3. Ore enrichment models

Rayleigh distillation is a classic model used in geochemistry to explain the enrichment of trace elements in crystalline rocks. The basic model considers the solidification of a magma to form the crystallizing solid. If an incremental mass of magma  $\delta M$  crystallizes, the incremental mass of mineral  $\delta M_m$  transferred from the magma to the solid is given by

$$\frac{\delta M_m}{M_m} = K \frac{\delta M}{M} \quad (8)$$

where  $M$  is the mass of magma,  $M_m$  is the mass of the mineral in the magma, and  $K$  is the solid–liquid partition coefficient. If the mineral is incompatible with the crystalline solid, we have  $K < 1$  and the remaining magma is systematically enriched. The smaller the value of  $K$ , the greater the enrichment is.

We can write Eq. (8) as a differential equation in the form

$$\frac{dM_m}{M_m} = K \frac{dM}{M} \quad (9)$$

Integrating with the condition that  $M_m = M_{m0}$  when  $M = M_0$  gives

$$\frac{M_m}{M_{m0}} = \left( \frac{M}{M_0} \right)^K \quad (10)$$

The mean concentration of the mineral in the enriched residual magma  $\bar{C}$  and the concentration of the mineral in the original magma  $C_0$  are given by

$$\bar{C} = \frac{M_m}{M} \quad (11)$$

and

$$C_0 = \frac{M_{m0}}{M_0} \quad (12)$$

Substitution of Eqs. (11) and (12) into Eq. (10) gives

$$\frac{\bar{C}}{C_0} = \left( \frac{M_0}{M} \right)^{1-K} \quad (13)$$

Comparing this result with Eqs. (5) and (7), we see that we have a fractal relation with a fractal dimension

$$D = 3K \quad (14)$$

The fractal dimension  $D$  is simply three times the solid–liquid partition coefficient  $K$ . This is consistent with the Menger sponge model illustrated in Fig. 2. If  $D = 3$ , the concentration is constant independent of scale which is consistent with  $K = 1$ . Allègre and Lewin (1995) and Turcotte (1997) have shown that the above analysis is also applicable to the chromatographic model.

### 4. Self-affine fractals

A second fractal approach to the analysis of data is the use of self-affine fractals (Malamud and Turcotte, 1999). Applications of self-affine fractals are to time series or to spatial distributions of data in one or more dimensions. An example would be the concentration of a mineral as a function of depth in a drill core. Self-affine fractal data analyses can also be applied to two-dimensional and three-dimensional data. Either the surface concentrations of a mineral or the full three-dimensional concentration distributions can be considered.

A standard approach to the analysis of a one-dimensional spatial data set  $c_i(x_i)$  is to carry out a Fourier transform of the data set. The spectral coefficients  $C_j(k_j, L)$ ,  $k_j$  wave number and  $L$  track length, are generally complex numbers indicating the amplitude and the phase of the signal. The standard measure of the spectral content of a signal is the spectral power density defined by

$$S_j(k_j) = \frac{1}{L} \left| C_j(k_j, L) \right|^2 \quad (15)$$

in the limit  $L \rightarrow \infty$ . A time series is self-affine if

$$S_j(k_j) = \nu k_j^{-\beta} \quad (16)$$

where  $\nu$  is a constant and the power  $\beta$  generally takes values in the range  $-1 \leq \beta < 3$ .

One classic data set is a Gaussian white noise. Each value in the data set is randomly picked from a Gaussian distribution of values. Adjacent values in the data set are uncorrelated and the spectral content is flat,  $\beta=0$  in Eq. (16). A second classic data set is a Brownian walk. A Brownian walk is obtained by taking the running sum of a Gaussian white noise. A Brownian walk is not stationary because its standard deviation  $\delta$  increases with increasing track length  $L$  according to  $\delta \sim L^{1/2}$ . A Brownian walk is scale-invariant and satisfies Eq. (16) with  $\beta=2$ .

The concepts of fractional Gaussian noises and fractional Brownian walks were introduced by Mandelbrot and Wallis (1968, 1969a,b). Fractional Gaussian noises are self-similar data sets that satisfy Eq. (16) with  $-1 \leq \beta \leq 1$ . These data sets are stationary in that the standard deviation  $\delta$  is not a function of the period  $T$ . In the range  $0 < \beta \leq 1$ , the fractional noise data sets are weakly persistent, adjacent values are positively correlated. In the range  $-1 < \beta < 0$ , the fractional noise data sets are weakly antipersistent, adjacent values are negatively correlated. Fractional Brownian walks are self-similar data sets that satisfy Eq. (16) with  $1 < \beta < 3$ . The running sum of a fractional Gaussian noise with  $\beta = \beta_g$  is a fractional Brownian walk with  $\beta_w = \beta_g + 2$ . Fractional Brownian walks are nonstationary with the standard deviation  $\delta(T)$  given by

$$\delta(T) \sim T^{Ha} \quad (17)$$

where  $Ha$ , the Hausdorff measure, is related to  $\beta$  by

$$Ha = \frac{\beta - 1}{2} \quad (18)$$

This relation is valid in the range  $1 < \beta < 3$ . An alternative approach to the analysis of self-similar fractional Gaussian noises was developed by Hurst et al. (1965). Their rescaled-range ( $R/S$ ) analysis was based on taking the variance of a running sum of the data set. The Hurst exponent  $Hu$  is related to  $\beta$  by

$$Hu = \frac{\beta + 1}{2} \quad (19)$$

and is valid in the range  $-1 < \beta < 1$ .

There are many geological and geophysical observations that are self-affine fractals to a good approximation (Pelletier and Turcotte, 1999). Topography on the Earth, moon, Venus, and Mars is well approximated by a Brownian walk ( $\beta=2$ ). Hurst et al. (1965) showed that time series of river discharges, lakes levels, thicknesses of tree rings and varves, and atmospheric temperature and pressure give Hurst exponents  $Hu \approx 0.75$  ( $\beta \approx 0.5$ ). Well logs are often self-similar data sets with  $\beta \approx 1$  (Todoschuck et al., 1990; Pelletier and Turcotte, 1996).

A number of authors have shown that mineral textures and distributions are fractal. Fowler (1990, 1995) quantified the mineral textures of igneous rocks using fractal techniques. Fowler et al. (1989) considered fractal and non-fractal features of disequilibrium silicate mineral textures. Bolviken et al. (1992) considered the fractal nature of geochemical landscapes. Cheng et al. (1994) used fractal techniques to separate geochemical anomalies from background noise. Zheru et al. (2001) quantified the fractal distribution of element distributions on mineral surfaces.

As an example of self-affine fractal composition distributions, we will consider the global distributions of lunar compositions as given by Feldman et al. (2002). Five global distributions are considered and each is expanded in spherical harmonics out to degree and order 30. The distributions considered are: (1) the abundance of thorium (Th), (2) the abundance of FeO (FeO), (3) the ratio of epithermal to fast neutrons ( $E/T$ ), (4) the flux of fast neutrons (FN), and (5) the visible albedo from the 750 nm wavelength band (albedo). The

harmonic amplitude  $A_i$  corresponding to degree  $\ell_i$  is given as a function of degree  $\ell_i$  in Fig. 5. The harmonic amplitude  $A_i$  is equivalent to the spectral coefficient  $C_i$ . From Eq. (15) we conclude that the power spectral densities  $S_i$  are proportional to the square of the harmonic amplitude  $A_i$ . Since the degree

$\ell_i$  is proportional to the wave number  $K_i$ , we can rewrite Eq. (16) as

$$A_i = C \ell_i^{-\beta/2} \quad (20)$$

The five straight-line correlations given in Fig. 5 correspond to Eq. (20) with  $\beta = 1.48$  (fast neutrons),

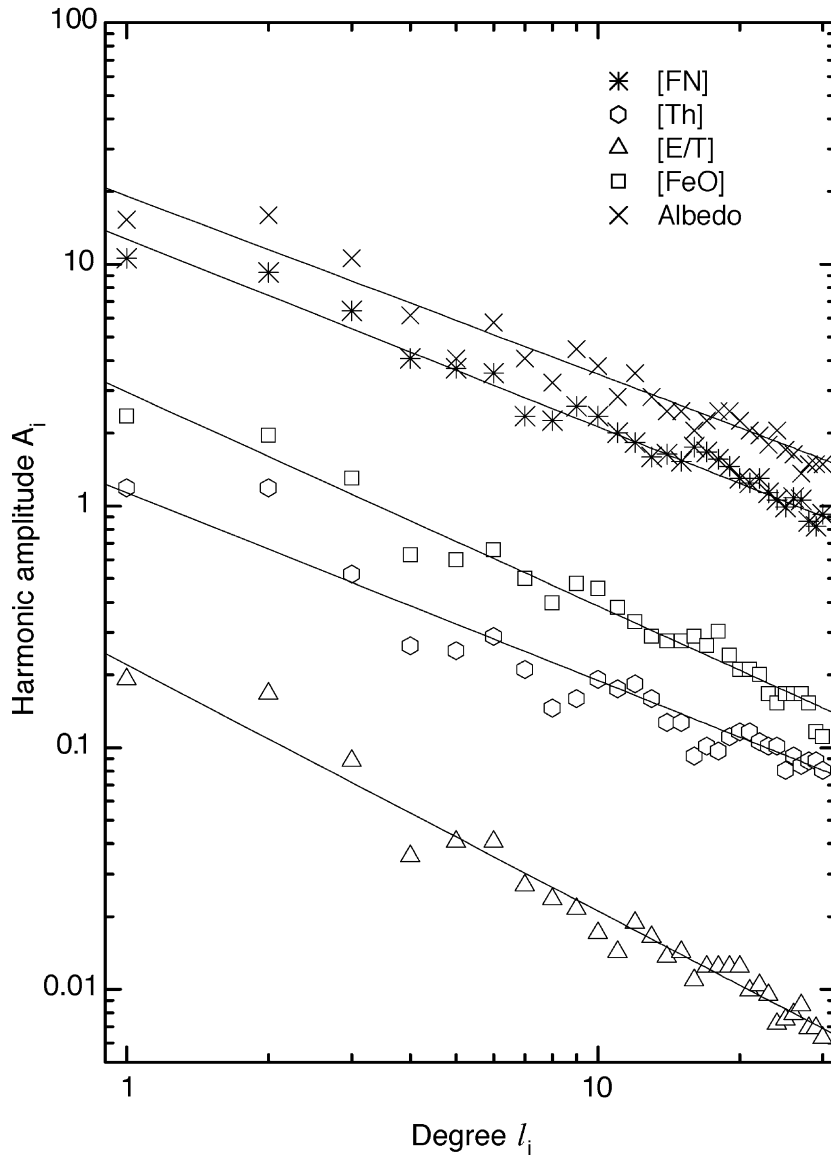


Fig. 5. Dependences of the harmonic amplitude  $A_i$  on the degree  $\ell_i$  for global compositional distributions on the moon (Feldman et al., 2002). Distributions considered are the thorium abundance (Th), FeO abundance (FeO), ratio of epithermal to fast neutrons ( $E/T$ ), flux of fast neutrons (FN), and the lunar albedo (albedo). Each distribution has been expanded in spherical harmonics to degree and order 30. The straight lines are from Eq. (20) taking  $\beta = 1.48$  (FN), 1.54 (Th), 1.72 ( $E/T$ ), 1.52 (FeO), and 2.04 (albedo).

$\beta = 1.54$  (thorium),  $\beta = 1.72$  (epithermal/thermal),  $\beta = 1.52$  (FeO), and  $\beta = 2.04$  (albedo). We see that all five measures of composition correlate quite well with the self-affine fractal relation (20).

## 5. Models for self-affine fractal behavior

Self-affine fractal behavior is found in a variety of geological and geophysical applications. The best known is planetary topography and bathymetry. Global topography satisfies Eq. (20) to a good approximation with  $\beta \approx 2$  (Turcotte, 1997, pp. 168–170), i.e., it is a Brownian walk as described above. Porosity variations in sedimentary basins are self-affine fractals to a good approximation both horizontally with  $\beta \approx 2$  and vertically with  $\beta \approx 1.5$  (Pelletier and Turcotte, 1996). Family (1986) provided an explanation for this behavior by using a stochastic diffusion model. Diffusion equations with Gaussian white-noise drivers give this type of behavior (Pelletier and Turcotte, 1999). Since the movement of minerals in petrology is often governed by the diffusion equation, random deposition plus diffusion can explain self-affine mineral distributions.

## 6. Multifractals

A third fractal approach to the analysis of data is to use multifractals (Turcotte, 1997). The simplest approach to illustrating the multifractal approach is to consider  $N$  points distributed along a line of length  $R$ . The line is divided into  $n$  segments of length  $r$  ( $n=1:r=R$ ,  $n=2:r=R/2$ ,  $n=4:r=R/4$ , and so forth). The probability  $p_{in}$  is the probability that a point is found in the  $i$ th line segment,  $i = 1, 2, \dots, n$

$$p_{in} = \frac{N_{in}}{N} \quad (21)$$

with

$$\sum_{i=1}^n p_{in} = 1 \quad (22)$$

The generalized moment of this distribution is defined by

$$M_q(r) = \sum_{i=1}^n p_{in}^q \quad (23)$$

which is valid for all values of  $q$  except  $q=1$ .

A distribution is multifractal if the generalized moments satisfy the scaling relation

$$M_q = Cr^{(q-1)D_q} \quad (24)$$

where the fractal dimensions  $D_q$  form the multifractal spectrum. For the self-similar fractal distributions considered above, all values of  $D_q$  are equal. The multifractal approach can be applied to continuous as well as discrete distributions in one, two, or three dimensions. The approach can also be applied to the analysis of time series. The applications of multifractal concepts have advantages but also disadvantages. The applicability of multifractal statistics to a natural process may provide important information on the underlying physical processes, multifractals are often associated with multiplicative cascades. However, multifractal statistics are much less useful than monofractal statistics from a practical point of view. A monofractal distribution (1) requires only two constants,  $D$  and  $\gamma$ . But a full multifractal spectrum requires an infinite number of constants. Monofractality implies scale invariance, multifractality does not. A log-normal distribution can be multifractal.

Agterberg (1995) applied multifractal modeling to the sizes and grades of giant and supergiant ore deposits. Goncalves (2001) applied multifractal modeling to geochemical distributions. Muller (1992) carried out multifractal characterizations of petrophysical data.

## 7. Conclusions

Fractal distributions are the only distributions applicable to scale-invariant processes. Many phenomena in petrology have one or more well-defined scales: interatomic spacings, crystal structure, grain size, defects, etc. Fractal concepts are not applicable in these cases. However, there are a variety of problems in petrology that do exhibit scale-invariance, at least over a range of scales. An important example is the distributions of concentrations of trace elements. The extreme values of

these concentrations lead to ore deposits. There is observational evidence that tonnage–grade data for at least some minerals are well approximated by fractal (power-law) distributions.

A major question in many branches of the earth sciences is whether extreme values have thin tails (exponential, log-normal) or fat tails (power-law, fractal). The choice of an applicable distribution can make orders of magnitude difference in extrapolating predictions to extreme values. Estimates of ore reserves are an example.

Spatial distributions of composition can be analyzed using the concept of self-affine fractals. The standard approach is to take a Fourier transform of the composition along a linear track. If the Fourier coefficients scale as a power-law of the wavelength, the distribution is a self-affine fractal. Stochastic differential equations can generate such distributions. An example is the Langevin equation, the diffusion equation with a random (Gaussian white noise) input.

Multifractal analyses can also be applied to problems in petrology. But multifractality does not necessarily imply scale invariance. However, evidence of multifractality is often taken to imply the applicability of a multiplicative cascade. Multiplicative cascades associated with log-normal distributions have been proposed as models for the concentrations associated with ore deposits (Ahrens, 1954a,b, 1963a,b).

Fractal concepts are widely used in many branches of geology and geophysics. But applications in petrology are relatively few. It is expected that many petrological measurements are and will be scale invariant for the same reasons that this is true in structural geology and sedimentology. Fundamental explanations of scale invariant behavior are also available as described in this paper.

## Acknowledgements

The author would like to thank Eric Lewin for a very constructive and helpful review.

## References

- Agerberg, F.P., 1995. Multifractal modeling of the sizes and grades of giant and supergiant deposits. *Int. Geol. Rev.* 37, 1–8.
- Ahrens, L.H., 1954a. The lognormal distribution of the elements (a fundamental law of geochemistry and its subsidiary). *Geochim. Cosmochim. Acta* 5, 49–73.
- Ahrens, L.H., 1954b. The lognormal distribution of the elements—II. *Geochim. Cosmochim. Acta* 6, 121–131.
- Ahrens, L.H., 1963a. Lognormal-type distributions in igneous rocks—IV. *Geochim. Cosmochim. Acta* 27, 333–343.
- Ahrens, L.H., 1963b. Lognormal-type distribution in igneous rocks—V. *Geochim. Cosmochim. Acta* 27, 877–890.
- Allègre, C.J., Lewin, E., 1995. Scaling laws and geochemical distributions. *Earth Planet. Sci. Lett.* 132, 1–13.
- Blenkinsop, T., 1994. The fractal distribution of gold deposits: two examples from the Zimbabwe Archean Craton. In: Kruhl, J.H. (Ed.), *Fractals and Dynamic Systems in Geoscience*. Springer-Verlag, Berlin, pp. 248–258.
- Bolviken, B., Stoeck, P.R., Jossang, T., 1992. The fractal nature of geochemical landscapes. *J. Geochem. Exp.* 43, 91–109.
- Cargill, S.M., 1981. United States gold resource profile. *Econ. Geol.* 76, 937–943.
- Cargill, S.M., Root, D.H., Bailey, E.H., 1980. Resources estimation from historical data: mercury, a test case. *J. Int. Assoc. Math. Geol.* 12, 489–522.
- Cargill, S.M., Root, D.H., Bailey, E.H., 1981. Estimating usable resources from historical industrial data. *Econ. Geol.* 76, 1081–1095.
- Carlson, C.A., 1991. Spatial distribution of ore deposits. *Geology* 19, 111–114.
- Cheng, Q., Agerberg, F.P., Ballantyne, S.P., 1994. The separation of geochemical anomalies from background by fractal methods. *J. Geochem. Exp.* 51, 109–130.
- Family, F., 1986. Scaling of rough surfaces: effects of surface diffusion. *J. Phys. A* 19, L441–L446.
- Feldman, W.C., Gasnault, O., Maurice, S., Lawrence, D.J., Elphic, R.C., Lacey, P.J., Binder, A.B., 2002. Global distribution of lunar composition: new results from Lunar Prospector. *J. Geophys. Res.* 107, E3-5-14.
- Fowler, A.D., 1990. Self-organized mineral textures of igneous rocks: the fractal approach. *Earth-Sci. Rev.* 29, 47–55.
- Fowler, A.D., 1995. Mineral crystallinity in igneous rocks—fractal methods. In: Barton, C., La Pointe, P. (Eds.), *Fractals in the Earth Sciences*. Plenum, New York, pp. 237–249.
- Fowler, A.D., Stanley, H.E., Daccord, G., 1989. Disequilibrium silicate mineral textures: fractal and non-fractal features. *Nature* 341, 134–138.
- Goncalves, M.A., 2001. Characterization of geochemical distribution: using multifractal models. *Math. Geol.* 33, 41–61.
- Harris, D.P., 1984. *Mineral Resources Appraisal*. Oxford Univ. Press, Oxford.
- Hurst, H.E., Black, R.P., Simaika, Y.M., 1965. *Long-Term Storage*. Constable, London.
- Korvin, G., 1992. *Fractal Models in the Earth Sciences*. Elsevier, Amsterdam.
- Lasky, S.G., 1950. How tonnage and grade relations help predict ore reserves. *Eng. Min. J.* 151, 81–85.
- Malamud, B.D., Turcotte, D.L., 1999. Self-affine time series: I. Generation and analyses. *Adv. Geophys.* 40, 1–90.
- Mandelbrot, B.B., 1967. How long is the coast of Britain? *Stat-*

- istical self-similarity and fractional dimension. *Science* 156, 636–638.
- Mandelbrot, B.B., Wallis, J.R., 1968. Noah, Joseph, and operational hydrology. *Water Resour. Res.* 4, 909–918.
- Mandelbrot, B.B., Wallis, J.R., 1969a. Computer experiments with fractional Gaussian noises, Parts I, II, III. *Water Resour. Res.* 5, 228–267.
- Mandelbrot, B.B., Wallis, J.R., 1969b. Robustness of the rescaled range  $R/S$  in the measurement of noncyclic long run statistical dependence. *Water Resour. Res.* 5, 967–988.
- Muller, J., 1992. Multifractal characterization of petrophysical data. *Physica A* 191, 284–288.
- Musgrove, P.A., 1965. Lead: grade–tonnage relation. *Min. Mag.* 112, 249–251.
- Pelletier, J.D., Turcotte, D.L., 1996. Scale-invariant topography and porosity variations in sedimentary basins. *J. Geophys. Res.* 101, 28165–28175.
- Pelletier, J.D., Turcotte, D.L., 1999. Self-affine time series: II. Applications and models. *Adv. Geophys.* 40, 91–166.
- Todoeschuck, J.P., Jensen, O.G., Labonte, S., 1990. Gaussian scaling noise model of seismic reflection sequences: evidence from well logs. *Geophysics* 55, 480–484.
- Turcotte, D.L., 1986. A fractal approach to the relationship between ore grade and tonnage. *Econ. Geol.* 81, 1528–1532.
- Turcotte, D.L., 1997. *Fractals and Chaos in Geology and Geophysics*, 2nd ed. Cambridge Univ. Press, Cambridge.
- Vistelius, A.B., 1960. The skew frequency distributions and the fundamental law of the geochemical processes. *J. Geol.* 68, 1–22.
- Zheru, Z., Huahei, M., Cheng, Z., 2001. Fractal geometry of element distribution on mineral surfaces. *Math. Geol.* 33, 217–228.